RSC Advances

RSC Publishing

REVIEW

View Article Online
View Journal | View Issue

Conjugated main-group polymers for optoelectronics

Xiaoming He and Thomas Baumgartner*

Cite this: *RSC Advances*, 2013, **3**, 11334

Received 19th January 2013,
Accepted 19th March 2013

DOI: 10.1039/c3ra40286j

www.rsc.org/advances

The last decade has witnessed great progress in conjugated polymers for application in optoelectronics. The biggest driving force for the field is to develop polymers with suitable HOMO and LUMO orbital energies, as well as high charge carrier mobility for improved performance in practical devices. Apart from the conventional donor–acceptor (D–A) strategy to tune the optoelectronic properties, the incorporation of main-group elements represents a promising new way to achieve a similar function, however, more efficiently, due to the intrinsic electronic properties of the main-group components. This review highlights the recent advances in main-group element-based conjugated polymers for application in optoelectronics, representatively focusing on Se-, Te-, P-, Si-, Ge-, and B-containing materials.

1. Introduction

Organic π-conjugated polymers are an important class of semiconducting materials that have been the focus of intense research over the past few decades, particularly with regard to applications in next-generation optoelectronic devices, such as organic photovoltaic cells (OPVs), organic light-emitting diodes (OLEDs) and organic field-effect transistors (OFETs).[1–9] Compared to 'traditional' inorganic silicon-based materials, these organic polymeric materials have unique advantages such as low cost and excellent solution processability, in addition to being light-weight. In this context, polythiophenes, polycarbazoles, polyfluorenes and poly(phenylene vinylene)s are noteworthy classes of conjugated materials that have been widely and successfully used in organic devices.[2]

While the above-mentioned materials have indeed shown considerable promise for practical applications, the development of new polymers with high charge carrier mobility, as well as suitable highest occupied molecular orbital (HOMO) and lowest unoccupied molecular orbital (LUMO) energy levels continues to be an active research direction, particularly for further improvement of the device performance.[4–8] One of the most widely used strategies for controlling the optoelectronic properties of organic conjugated polymers is the molecular engineering of the combination of electron-donating (D) and electron-accepting (A) building blocks in the conjugated backbone.[5,6] Especially for application in organic photovoltaics, the polymer should have a low energy gap to allow for

Department of Chemistry and Centre for Advanced Solar Materials, University of Calgary, 2500 University Dr NW, Calgary, Alberta, T2N 1N4, Canada. E-mail: Thomas.baumgartner@ucalgary.ca; Fax: +1 403-289-9488

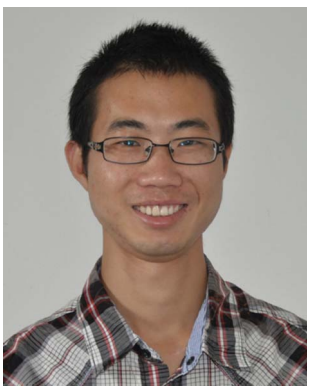

Xiaoming He

Xiaoming He received his M.Sc. under Shijun Shao at Lanzhou Institute of Chemical Physics, Chinese Academy of Science in 2006 and his Ph.D. in 2010 from the University of Hong Kong under the supervision of Vivian W. W. Yam. Then, he spent 1 year in the group of Mi Hee Lim's research group at the University of Michigan, working on the design of multifunctional small molecules as chemical probes and therapeutic agents for human neurodegenerative diseases. Since 2012, he is a postdoctoral fellow in the group of Thomas Baumgartner focusing on the development of novel organophosphorus electron-accepting materials.

Thomas Baumgartner

Thomas Baumgartner received his Ph.D. degree in 1998 from the University of Bonn, Germany working with Edgar Niecke. From 1999 to 2002 he was a postdoctoral fellow at the University of Toronto, Canada with Ian Manners. He started his independent research career at the Johannes Gutenberg-University in Mainz (2002–2003) and at the RWTH-Aachen University (2003–2006), both in Germany. In 2006 he joined the Department of Chemistry at the University of Calgary, Canada, where he currently is an Associate Professor. His research interests are focused on organophosphorus π-conjugated materials for organic electronics, as well as supramolecules and polymers.

better light-harvesting of the solar spectrum by covering a broader spectral range.[4–6] According to a model by Scharber and co-workers, the power conversion efficiencies (PCEs) of OPV devices consisting of a light-harvesting polymer and an electron-accepting fullerene derivative could potentially be improved to up to 10% by appropriately engineering the energy levels of the conjugated polymer.[10] The molecular engineering is usually accomplished *via* variation of substituents appended to the polymers' building blocks, or more effectively *via* modification of the atomic composition of the building blocks themselves. Along the same lines, the incorporation of inorganic main-group elements into π-conjugated materials has created a promising way for efficiently engineering the optoelectronic properties of conjugated materials, due to their very unique structural (*i.e.*, bonding) and electronic properties.

In this review, we present the recent efforts in improving the properties of conjugated polymers for optoelectronics by means of incorporating main-group elements. We will representatively focus on the Group 16 elements selenium (Se) and tellurium (Te), the Group 15 element phosphorus (P), the Group 14 elements silicon (Si) and germanium (Ge), as well as the Group 13 element boron (B). These elements have been found to impact the materials' properties considerably and showcase the intriguing range of opportunities by utilizing main-group elements for this purpose most illustratively.

2. Selenium-containing polymers

Polythiophenes and related thiophene-containing polymers are a class of materials that have most frequently been used as conjugated materials in optoelectronic devices.[11,12] The combination of regioregular poly(3-hexylthiophene) (P3HT) and [6,6]-phenyl-C_{61}-butyric acid methyl ester ($PC_{61}BM$), or [6,6]-phenyl-C_{71}-butyric acid methyl ester ($PC_{71}BM$) has been a benchmark for OPVs for a long time, with average power conversion efficiencies (PCE) around 5% (Fig. 1).[13] However, these PCE values represent the ceiling for this class of materials, mainly due the limited absorption profile of the polythiophenes. In order to improve the PCE of OPV devices, enormous efforts have been focused on the development of new low-band gap polymers with improved light-harvesting properties that better match the sun's emission spectrum.

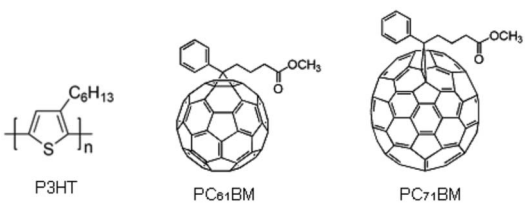

Fig. 1 Widely used electron-donor polymer poly(3-hexylthiophene) (P3HT) and electron-accepting fullerene derivatives $PC_{61}BM$ and $PC_{71}BM$ in OPVs.

Notably, many of these polymers are still based on thiophene building blocks that are used in a D–A approach and the topic has been extensively studied and is extremely well reviewed.[10,11]

Selenophene-containing polymers, on the other hand, have been developed in recent years in an alternative search for polymers with improved properties for practical applications.[11] On going from S to the heavier congener Se, the resulting polymers were found to indeed exhibit lower band gaps. Theoretical calculations showed that the HOMO in thiophene-based conjugated materials has no contribution from the sulfur, while the LUMO has a significant coefficient on the heteroatom.[14] Therefore, replacement of S with a heavier heteroatom, such as Se, would have a large influence on the LUMO, but not the HOMO energy. Due to the lower ionization potential of the heavier heteroatom, incorporation of Se into a polymer would lead to a lowered LUMO energy level, and therefore provide for a smaller energy gap than the corresponding thiophene-containing polymer.[14] While there have been several polymers reported that utilize selenophene instead of thiophene, it should be noted, however, that the majority of the work is still at its proof-of-concept stage and many results have not (yet) exceeded the sulfur-analogues in terms of performance. Most of these studies have nevertheless provided a crucial proof for the general feasibility of the approach.

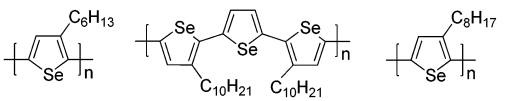

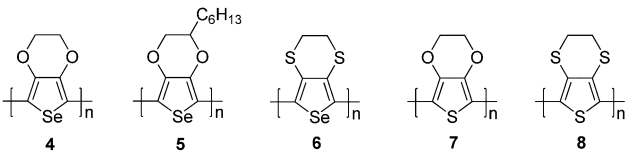

In 2007, Heeney and co-workers reported the selenium analogue of P3HT, regioregular poly(3-hexylselenophene) (P3HS, **1**).[14] This polymer has a smaller optical gap (1.6 eV) than regioregular P3HT (1.9 eV). Both P3HT and P3HS were shown to have the same HOMO level (4.8 eV), and the decrease in band gap was consequently attributed to a drop in the P3HS LUMO. In addition, both polymers have similar charge mobilities in corresponding field-effect transistors.

Ensuing, P3HS was demonstrated as a promising alternative to the corresponding polythiophenes for solar cell applications.[15] By decreasing the LUMO level of the donor while keeping the HOMO at the same level as P3HT, the reduced band gap would allow for a greater light-harvesting ability without compromising the open circuit voltage (V_{oc}) of the OPV device. An optimal device using $PC_{61}BM$ as the acceptor (50 wt% $PC_{61}BM$, blend film thickness 135 nm,

annealed at 150 °C), produced a PCE of 2.7%, close to that of a P3HT:$PC_{61}BM$ device measured under the same conditions.

In a slight variation of the structural motif found in P3HS, polyselenophenes **2** and **3**, have been developed and shown to be promising ambipolar organic semiconductors. Both polymers have the same optical band gap of 1.8 eV.[16] However, compared to their sulfur analogues, these polyselenophenes have smaller band gaps and lower LUMO levels, facilitating electron injection and electron transport. Polymer **2** even showed matching electron and hole mobilities on the order of μ = 0.03 $cm^2\ V^{-1}$ s. On the other hand, the electron mobility of polymer **3** was relatively low in the order of μ_e = 0.004–0.009 $cm^2\ V^{-1}$ s, which was attributed to the larger injection barrier and/or shorter conjugation length. Overall, however, polyselenophenes have now been demonstrated to be a promising class of ambipolar organic semiconductors for applications in optoelectronic devices.

Along the same lines, Bendikov and co-workers have reported a family of 3,4-disubstituted polyselenophenes **4**–**6**.[17–20] This interesting topic has been reviewed recently and we will therefore only highlight some representative examples in this review.[21] They developed a new and efficient method for the preparation of various 3,4-disubstituted selenophene monomers, such as 3,4-ethylenedioxyselenophene (EDOS),[17] hexyl-3,4-ethylenedioxyselenophene (EDOS-C6)[18] and 3,4-ethylenedithioselenophene (EDTS)[20] from commercially available 2,3-dimethoxy-1,3-butadiene, as shown in Scheme 1. As a selenium analogue of poly(3,4-ethylenedioxythiophene) (**7**) that is a very important conducting polymer used in many electronic devices, the band gap of poly(3,4-ethylenedioxyselenophene) (**4**) was determined to be 1.4 eV, which is 0.2 eV lower than **7**.[17] In addition, PEDOS exhibited a high conductivity of *ca.* 3–7 S cm^{-1}, which is promising for the field of conductive polymers.

The same group also demonstrated that polyselenophenes have excellent electrochromic properties.[18,19] Polymer **4** exhibits a high contrast ratio of 55% at 666 nm (λ_{max}) and a coloration efficiency of 212 $cm^2\ C^{-1}$. The effect of the alkyl chains on the conjugated backbone on the electrochromic properties has also been investigated. Polymer **5** with hexyl group shows the best performance, exhibiting a high contrast ratio of 88–89%, a high coloration efficiency of 773 $cm^2\ C^{-1}$, and a fast switching time at a low switching voltage of −0.9 to 0.5 V. As shown in Fig. 2, the film of **5** can dramatically change its color by switching between the neutral state (pure-blue) and oxidized state (colourless). At an applied potential of −0.9 V, the neutral form of the polymer shows a distinctive π to π* transition with λ_{max} = 686 and 763 nm and one shoulder peak at 632 nm. As the applied potential increases, the original absorption peaks decrease, while the polaron (1100 nm) and bipolaron peaks (that peak in the NIR beyond the limits of the spectrophotometer) increase.

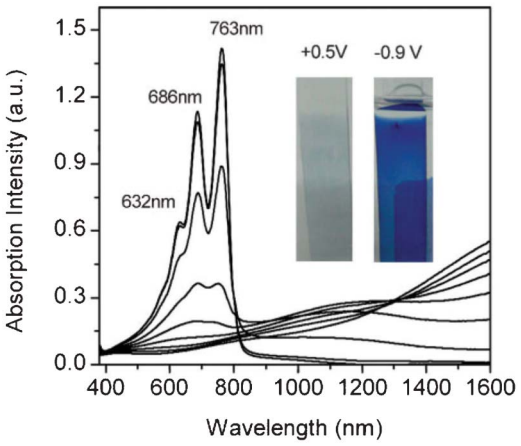

Fig. 2 Spectroelectrochemical spectra of polymer **5**. Adapted with permission from ref. 18.

In addition, oligo- and polyselenophenes have been demonstrated to be a class of important materials that can control the planarity in conjugated polymers.[20] Compared with **8**, polyselenophene **6** shows greater degree of planarity and significant narrower optical band gap (ΔE_g = 0.6–0.8 eV). X-Ray crystal structures show that bis(3,4-ethylenedithioselephene) (**9**) has a high planarity, which is complete contrast to its thiophene counterpart **10** that has a strong twist of 45° about the two thiophene planes. Theoretical calculations also suggest that the twisting of oligoselenophenes requires more energy than for their thiophene analogues, and therefore, they should maintain planarity with a wider range of substituents.

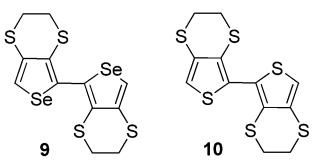

Interestingly, oligofurans, the oxygen-based congeners, also reported by Bendikov and co-workers, exhibit highly planar structures as well.[22] In addition, oligofurans have the advantages of higher fluorescence, tighter herringbone solid-state packing, greater rigidity and solubility than oligothiophenes.

In addition to the polyselenophenes, a range of selenophene-containing copolymers have been reported to show low-

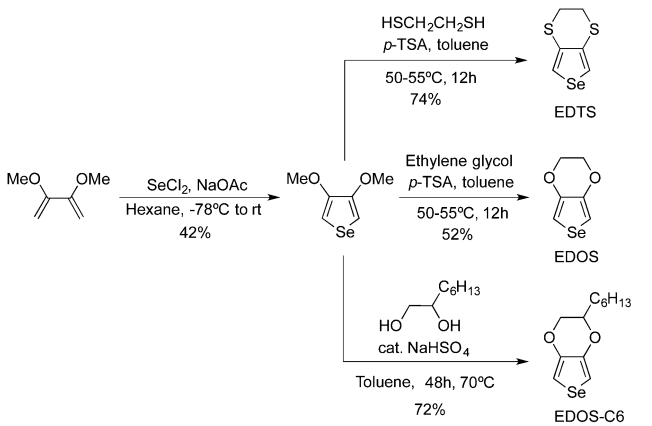

Scheme 1 Synthesis of EDTS, EDOS and EDOS-C6.

energy gaps, high charge mobilities and promising performance in solar cells. Park, Shim and co-workers reported two selenophene- and thiophene-containing copolymers **11** and **12**, and the investigation of their thin-film transistor (TFT) performance.[23] Polymer **11** exhibited a high hole mobility of μ_h = 0.02 $cm^2\ V^{-1}\ s$, while **12** exhibited a very poor hole mobility of only $\mu_h = 1.4 \times 10^{-5}\ cm^2\ V^{-1}\ s$. It was found that the differences resulted from the intermolecular ordering in the solid state. X-Ray diffraction (XRD) and atomic force microscopy (AFM) measurements in addition to theoretical calculations demonstrated that **11** showed highly ordered interlayer alignment and π-stacking that was absent for polymer **12**.

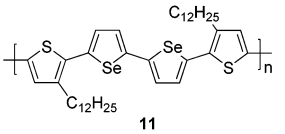

11

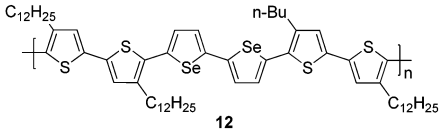

12

The groups of Heeney, Kronemeijer, and Sirringhaus subsequently developed a series of copolymers **13–16** containing selenophene and diketopyrrolopyrrole (DPP) units, as well as different bridging moieties, for the investigation of their field-effect transistor and OPV performance.[24–26] DPP was chosen because of its earlier successful utilization in conjugated polymers with high ambipolarity and good photovoltaic efficiencies.[27,28] The copolymers **13a** and **13b** that exhibit alternating thiophene- or selenophene-flanked DPP and benzothiadiazole were developed in 2012.[24] Consistent with earlier studies, substitution with selenophene results in a significant reduction of the optical band gap from 1.20 to 1.05 eV, and a red shift of the absorption maximum from λ_{max} = 923 nm to λ_{max} = 964 nm that can again be ascribed to a lowered LUMO level in the Se-containing congener. Polymer **13b** also showed excellent thermal stability, as well as high hole (μ_h = 0.46 $cm^2\ V^{-1}\ s$) and electron mobilities (μ_e = 0.84 $cm^2\ V^{-1}\ s$).

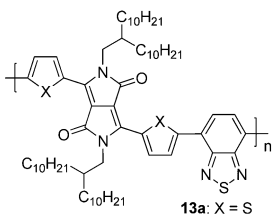

13a: X = S
13b: X = Se

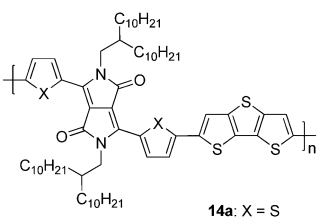

14a: X = S
14b: X = Se

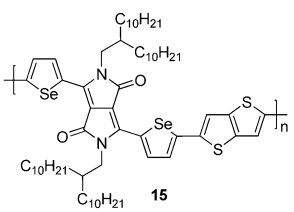

15

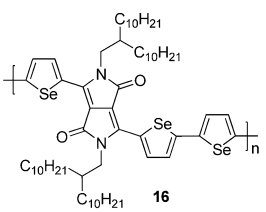

16

As continuing investigation into these selenophene-containing materials, copolymers **14a** and **14b** were subsequently developed.[25] Both polymers show a high ambipolar behavior in field-effect transistors. OPV devices utilizing these polymers in conjunction with $PC_{71}BM$ showed promising efficiencies of 5.10% and 4.05% for **14a** and **14b**, respectively. Very recently, Heeney and co-workers reported polymers **15** and **16**, which displayed high and balanced electron and hole mobilities over μ = 0.1 $cm^2\ V^{-1}\ s$.[26]

Yang and co-workers developed a novel ambipolar polymer **17** with unprecedentedly high hole (μ_h = 3.97 $cm^2\ V^{-1}\ s$) and electron (μ_e = 2.20 $cm^2\ V^{-1}\ s$) mobilities through a rational molecular design of both the conjugated backbone and the side chains.[29] The siloxane side chains can effectively control the intermolecular π–π stacking of the conjugated polymer, enhancing the charge transport. This strategy is very promising for tuning the charge transport of conjugated polymers by introduction of the siloxane side chains.

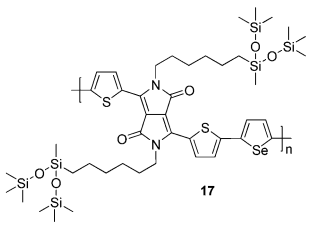

17

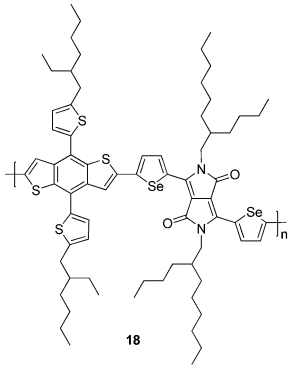

18

Very recently, the same group developed the low bandgap polymer **18** (E_g = 1.38 eV), which exhibited excellent photovoltaic performance, with a high photo-current of 16.8 mA cm^{-2} and a PCE of 7.2% in a single junction solar cell device.[30] Importantly, the new polymer significantly enhanced the tandem and visibly-transparent cell performance, with PCEs as high as 9.5% and 4.5%.

Seferos and co-workers recently reported a new type of block copolymer, poly(3-hexylselenophene)-*block*-poly(3-hexylthiophene) (P3HS-*b*-P3HT, **19**), and compared it with the statistical copolymer, and two homopolymers (P3HT and P3HS).[31] The structures of the polymers were confirmed by ^1H NMR and optical measurements. As shown in Fig. 3, the absorption of a film of **19** exhibits shoulders that coincide with the π-stacking bands of both P3HT and P3HS. AFM experiments clearly show the distinct domains, which are not observed in either the statistical copolymer or two homopolymers.

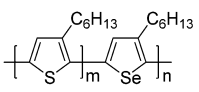

19

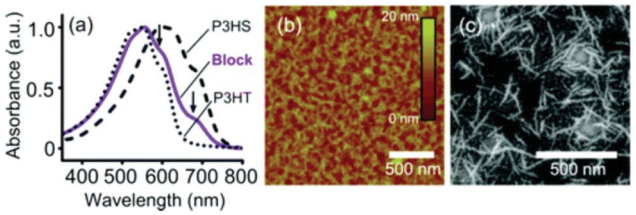

Fig. 3 (a) Absorbance spectrum, (b) AFM height image, and (c) darkfield STEM image of poly(3-hexylselenophene-*block*-3-hexylthiophene) (**19**) films. Reprinted with permission from ref. 31. Copyright 2010 American Chemical Society.

Based on the thin-film absorption and the AFM data, block copolymer **19** was confirmed to exhibit a significant degree of phase separation in the solid state.

3. Tellurium-containing polymers

Continuing the same trend on going from S to Se, incorporation of tellurium (Te) results in further narrowing of the energy gap in conjugated materials. In addition, Te tends to form strong Te–Te interactions, and therefore, Te-containing polymers should be capable of beneficial supramolecular interactions that lead to strong interchain electronic coupling and, consequently, to improved control over structure and properties. Due to its metalloid nature, Te-containing polymers have also been demonstrated to easily undergo post-polymerization modification by coordination of Br_2 to the Te centers resulting in further tuned optoelectronic properties. It should be mentioned however, that the examples of conjugated Te-containing materials are strictly limited, but the few examples of polytellurophenes have been summarized by Seferos *et al.* in a review paper in 2010[32] and representative species are therefore only briefly covered by this review.

In 2009, Bendikov and co-workers reported the synthesis and electropolymerization of 3,4-dimethoxytellurophene (**20**) (Scheme 2).[33] This was also the first investigation of the spectroscopic properties of a polytellurophene. The X-ray structure of **20** showed strong Te–Te interactions with a distance of 3.80–4.04 Å, which are shorter than the van der Waals distance of Te (4.30 Å). From the onset of absorption, the band gap of polymer **21** was determined to be 1.51 eV, which is about 0.2 eV lower than its selenophene analogue.

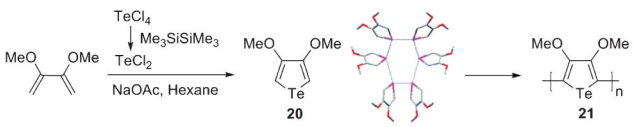

Scheme 2 Synthesis of 3,4-dimethoxytellurophene (**20**) and its X-ray crystal structure, as well as the electropolymerization to polymer **21**. Adapted with permission from ref. 33. Copyright 2009 American Chemical Society.

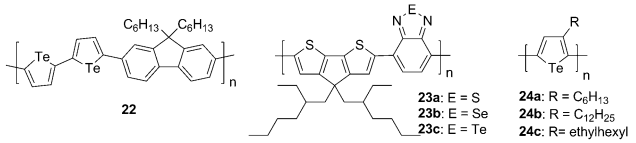

The poly(bitellurophene-alt-9,9′-dihexylfluorene) copolymer **22** was reported by Seferos and co-workers.[34] Access to the polymer was made possible *via* the new 5,5′-diiodo-bitellurophene monomer that was synthesized by reacting bitellurophene with *N*-iodosuccinimide (NIS). The choice of NIS avoids the production of Br_2, which can coordinate to the Te atom. Compared to the UV-vis absorption of bitellurophene at λ_{max} = 385 nm, the polymer exhibited a distinctly red-shifted absorption band at λ_{max} = 488 nm in $CHCl_3$ solution, indicating electronic delocalization along the polymer chain. On going from solution to the thin film, polymer **22** showed a further red shift in absorption to λ_{max} = 506 nm, indicative of increased order in the solid state. In addition, two shoulders at 540 and 610 nm were also observed in the absorption spectrum, suggesting further organization and π-stacking in the solid state, which is an important feature for solid-state electronic materials. Importantly, the photophysical properties of this polymer can be further tuned by Br_2 coordination. As shown in Fig. 4, addition of Br_2 leads to a red shift of the absorption maximum to λ_{max} = 552 nm, and an obvious color change from orange to purple, along with a significant red shift of the absorption onset from λ_{onset} = 624 to 727 nm. Furthermore, coordination of Br_2 resulted in the lowering of both the HOMO and LUMO energy levels. Interestingly, the Br_2 coordination is reversible, leading to the original divalent, debrominated Te-polymer upon annealing at 150 °C. Such Br_2 coordination to polytellurophene has not been observed for the thiophene and selenophene analogues, supporting its high specificity and highlighting the exceptional utility of tellurophene-containing polymers.

The same group also systematically studied the effect of S-, Se-, and Te-atom substitution on the optoelectronic properties in D–A polymers **23a–23c** by optical spectroscopy, solvatochromism, density functional theory (DFT), and time-dependent DFT calculations.[35] All of the polymers were found to have dual absorption bands, containing low- and high-energy

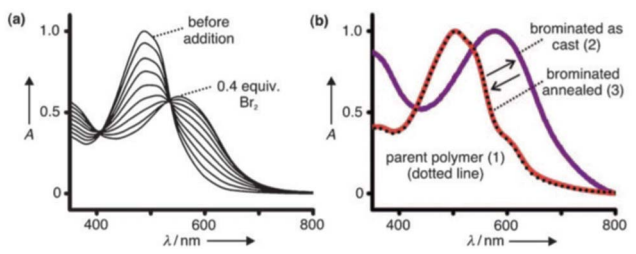

Fig. 4 (a) Solution absorption spectra of **22** before and after addition of bromine. (b) Solid state absorption spectra of the parent polymer film, the brominated polymer film, and the brominated polymer film after annealing. Adapted with permission from ref. 34.

optical transitions. Substitution by a heavier atom leads to a red shift in the low-energy transition, while the high-energy band remains relatively constant in energy. Based on the absorption onsets, the band gaps of the polymers were determined to be 1.59, 1.46, and 1.06 eV for the S-, Se-, and Te-containing species, respectively. In addition, the intensity of the low-energy absorption band decreased, while the high-energy band remained the same. The red shift in the low-energy absorption was attributed to both a decrease in ionization potential and a decrease in the acceptor aromaticity. The loss of intensity of the low-energy band was explained by the decrease in electronegativity of the acceptor. This groundbreaking Te-polymer research has provided some intriguing insights on the potential of heavy main group elements by introducing a new method of controlling the optical properties of D–A polymers by single atom substitution into the acceptor.

Very recently, Seferos and co-workers also reported a series of poly(3-alkyltelluophene)s **24**.[36] Similar to polythiophenes, these polymers have the advantages of regioregularity and the ability to self-organize in solid state. As expected, these polymers showed red-shifted optical properties (λ_{max} = 558 and 545 nm for **24a** and **24b**) and a narrow energy band gap (E_g = 1.44 and 1.57 eV for **24a** and **24b**). It can be expected that this research will open up a wide range of future studies in the field of organic electronics.

4. Phosphorus-containing polymers

The incorporation of phosphorus centers in conjugated polymers offers promising optical and electronic properties because of the versatile reactivity and physical properties of this Group 15 element. Among organophosphorus materials, phosphole-based systems have attracted significant attention.[37–43] In contrast to the N-center in its lighter congener pyrrole, the phosphorus atom in phosphole adopts a pyramidal geometry, which leads to insufficient n–π interaction and considerably reduced aromaticity in the P-system. In terms of building blocks, the basic phosphole as well as the fused dithienophosphole and dibenzophosphole are the most studied frameworks for the development of functional conjugated materials (Fig. 5). Extensive groundbreaking studies by the Réau group, our group, and others have highlighted the exceptional fine-tuning opportunities for the optical and electronic properties by simple and efficient chemical modification of the phosphorus center. In addition, the presence of the phosphorus center was found to increase the electron-acceptor properties of these materials as a result of an σ*–π* interaction between the exocyclic substituent and the π-conjugated scaffold that is made possible by the strongly pyramidal nature of P (Fig. 5b), thereby providing an excellent conduit for the generation of n-type conjugated materials.[44,45] Consequently, phosphole-based species were identified as highly desirable building blocks for the generation of

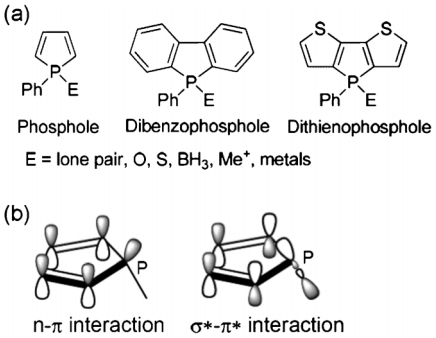

Fig. 5 (a) Structures of phosphole derivatives (b) orbital interactions (n–π and σ*–π* interaction) in phospholes.

conjugated molecules and polymers for application in organic electronics.

Although Mathey and co-workers reported the first efforts toward phosphole-based oligomers by sequential lithiation and oxidation coupling with $CuCl_2$ as early as 1994,[46] the first real, well defined polyphosphole **25** was only reported by Matano and co-workers in 2010.[47] The UV-vis absorption of **25** displays an intense absorption band at λ_{max} = 655 nm, which is strongly red-shifted relative to its model compounds (mono-, di- and trimer). From the absorption onset at λ_{onset} = 850 nm, the energy gap of **25** was determined to be 1.46 eV. While the monomer is emissive (ϕ_{PL} = 0.19), the dimer and trimer were found to be only weakly emissive ($\phi_{PL} < 0.02$), and the polymer turned out to be non-emissive. Notably however, the electron-accepting character of the phosphole is significantly enhanced in the polymer. It should also be noted in this context that the first phosphole-containing copolymer **26** was reported by Tilley and co-workers in 1997.[48] The group utilized the zirconocene diyne-coupling as a general approach to afford the zirconacyclopentadiene polymer, followed by the reaction with dichlorophosphane to get the P-polymer as an air-sensitive, soluble, yellow solid. The ultimately ill-defined polymer, due to lack of regiochemical control during alkyne-coupling, exhibited a UV-vis absorption maximum at λ_{max} = 308 nm, and a blue emission at λ_{em} = 470 nm with a quantum yield of ϕ_{PL} = 0.092.

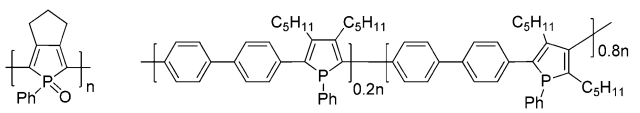

Since 2000, Réau and co-workers have extensively studied the electropolymerization of the 2,5-bis(2-thienyl)phosphole derivatives **27a–27e**.[49–51] The electropolymerization was found to strongly depend on the electronic nature of the phosphorus center. The trivalent σ^3-phosphole **27a** did not tolerate the oxidation process to form polymer **28a**, which was ascribed to the possibility of the nucleophilic reaction of the P atom with the radical cations or protons during the chain-growth process. By contrast, monomers **27b–27e**, modified with O, S, Se or AuCl, respectively, did electropolymerize well to form

films on a Pt electrode. The E_{pa} values of the corresponding polymers were reported to depend on the nature of the P-substituent (E). Interestingly, polymer **28a** could be easily accessed by Au-deprotection of the P center in **28e**. This transformation was accompanied by a significant negative shift in the oxidation current offset and a blue shift of the UV-vis absorption, indicative of the strong electronic coupling of the P moieties with the π-conjugated polymeric backbone. Moreover, the versatile reactivity of the trivalent phosphole moieties also allows for **28a** to be utilized in the sensing of elemental chalcogenides. Similarly relevant polymers **29** and **30** were also synthesized by electropolymerization.[52]

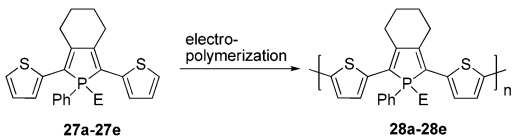

27a-27e **28a-28e**

E = lp (**a**), O (**b**), S (**c**), Se (**d**), AuCl (**e**)

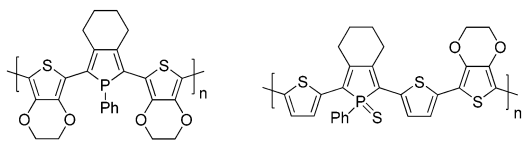

29 **30**

Chujo and co-workers utilized Sonagashira coupling to chemically access a variety of conjugated polymers (**31a–31e**) that were based on the Réau phosphole monomer with various aryl moieties as spacers.[53–55] These polymers generally emit at λ_{em} = 460–520 nm with quantum yields in the range of ϕ_{PL} = 0.13–0.39.

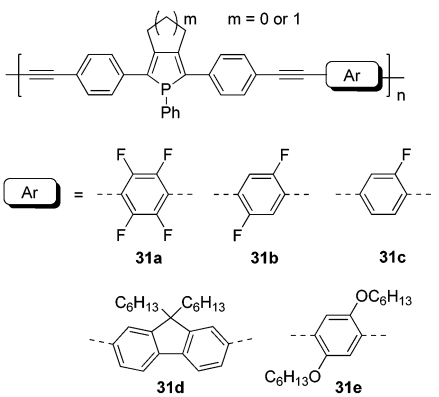

31a **31b** **31c**

31d **31e**

The dithienophosphole system (Fig. 5), developed by our group since 2004, has extraordinary photophysical properties that can also be easily tuned by phosphorus modification and π-extension of the basic core.[56–58] The parent core is a strong blue-light emitter with photoluminescence efficiencies of up to 90%, suggesting its suitability for optoelectronic, as well as sensing applications.[56] Very recently, our group has also reported a series of novel luminescent liquid crystals and organogels based on this building block, however, using molecular species.[59,60]

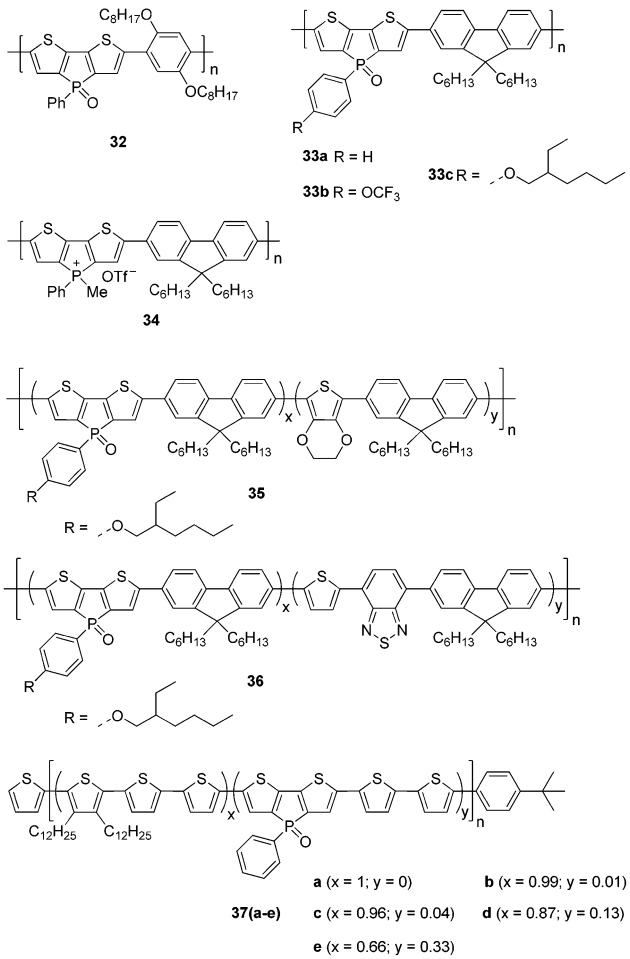

32 **33a** R = H **33b** R = OCF_3 **33c** R =

34

35 **36**

37(a-e) **a** (x = 1; y = 0) **b** (x = 0.99; y = 0.01) **c** (x = 0.96; y = 0.04) **d** (x = 0.87; y = 0.13) **e** (x = 0.66; y = 0.33)

The earliest attempt to access a dithienophosphole-containing polymer was achieved in 2004 by incorporating the dithienophosphole moiety as side group in a solution-processable polystyrene that exhibited very strong blue emission at 424 nm.[56] Although not a truly conjugated polymer, this study opened up potential applications of dithienophosphole-containing polymers in optoelectronic devices, such as blue-light emitting PLEDs and polymeric sensors.[56] A similar strategy was later successfully employed for generating white-light emission by incorporating two dithienophosphole luminophores as functional side groups in polystyrene.[61]

Our group also developed a series of dithienophosphole-containing conjugated polymers (**32–37**) with different alternating aromatic units.[57,58,62–64] The first example **32** showed intense emission in the green-yellow region with the maximum of λ_{em} = 555 nm, significantly red-shifted from the monomer (λ_{em} = 463 nm), indicating extended π-conjugation. Although the polymer showed limited solubility, this research clearly supported the possibility of building up dithienophosphole-containing π-conjugated polymers. Later on, various alternating aromatic units, different lengths of spacers, modification of the P center and introduction of solubilizing groups have been investigated in order to further tune the

photophysical properties and the solubility of the polymers. A series of dithienophosphole-fluorene copolymers (**33a–33c**), have been accessed by Suzuki–Miyaura coupling.[58,62] Polymers **33a–33c** exhibit strong photo-luminescence at λ_{em} = 545–550 nm with quantum yields in the range of ϕ_{PL} = 0.24–0.49.

Although neutral polymer **33a** still exhibited somewhat limited solubility, the cationic polymer **34** showed greatly increased solubility in organic solvents (*e.g.* $CHCl_3$, CH_2Cl_2, THF) and could also be isolated with higher molecular weights (*i.e.*, longer polymer chains). The photoluminescence of **34** in solution exhibited a maximum peak at λ_{em} = 509 nm with a shoulder at λ_{em} = 540 nm. The thin film showed a featureless but further red- shifted emission at λ_{em} = 556 nm, indicative of intermolecular interaction in the solid state. Contrary to many ''classic'' polyelectrolytes, such a strikingly strong fluorescence of **34** in the solid state was attributed to the steric bulk around the cationic phosphorus atoms that reduces the accessibility of these centers for potential quenchers in the solid state.

Introduction of the branched 2-ethylhexyl alkyl chain at the phosphole building block in **33c** provided improved solubility for the neutral polymers. This new building was also applied in two ABC-copolymers **35–36**. The photophysical properties of **35** (λ_{em} = 550 nm, ϕ_{PL} = 0.60) are similar to those of **33a–33c**. Polymer **36**, on the other hand, showed significantly red-shifted emission at λ_{em} = 658 nm (ϕ_{PL} = 0.46) in solution and λ_{em} = 695 nm in the solid state. The optical band gaps of **36** in solution and the solid state were determined to be 2.0 and 1.7 eV, respectively, indicating its potential for application as light-harvesting material in OPVs.

Recently, we reported a family of dithienophosphole-based polythiophenes **37a–37e** and presented a structure-property study by investigating the effect of dithienophosphole content on the photophysical and electrochemical properties. Solution emission spectra of all the polymers displayed similar maxima at approximately λ_{em} = 604–613 nm. The thin-film emission spectra underwent large red shifts with maxima at λ_{em} = 666–693 nm. Generally, increasing the content of dithienophosphole in polymers **37d** and **37e** led to red-shifted absorption and emission properties, as well as smaller band gaps. The reason was attributed to the desired effect of the electron-accepting dithienophosphole in lowering the LUMO energy levels by creating charge transfer states in the copolymer backbone.

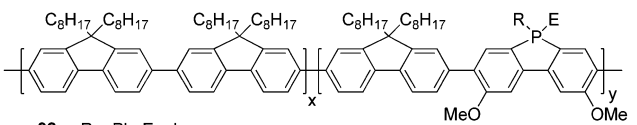

38a R = Ph, E = lp
38b R = C_4H_9, E = O

Dibenzophosphole, which can be considered the phosphorus analogue of fluorene and carbazole, has also been successfully introduced in conjugated polymers. Huang and co-workers reported two conjugated polymers **38a** and **38b** containing alternating fluorene and dibenzophosphole chromophores, and investigated their application in polymeric light-emitting diodes (PLEDs).[65] Both polymers showed

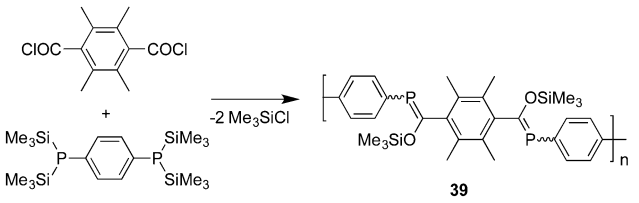

39

Scheme 3 Becker synthetic route to PPP.

unique optoelectronic properties. Polymer **38a** exhibited a blue electroluminescence (EL) (CIE = 0.21, 0.24) with emission maxima at 424, 450, and 478 nm, while the EL of the P-oxidized **38b** resulted in white-light emission (CIE = 0.34, 0.36). The P-modification-dependent EL performance highlights the great advantage of phosphorus-containing conjugated materials for optoelectronic devices.

The phosphorus analogues of poly(*p*-phenylene vinylene)s (PPVs) with P=C or P=P linkages along the polymer backbone, are new types of conjugated phosphorus-containing polymers with interesting electronic and spectroscopic properties.[40] In 2002, Gates and co-workers reported the first example of the conjugated poly(*p*-phenylene phosphaalkene) (PPP) polymer **39**, which they accessed synthetically *via* the Becker route (Scheme 3).[66] Both *Z*- and *E*-isomers were observed in a ratio of *ca.* 1 : 1 by ^{31}P NMR spectroscopy. Compared to its molecular model compounds, the UV-vis absorption of polymer **39** exhibited a red shift, indicating an extended π-conjugated system. Later, systematic research demonstrated that bulky substituents around the P center were crucial for the stability and in controlling the stereochemistry, resulting in mainly in *Z*-isomer.[67] The latter also exhibited improved π-conjugation over the isomeric mixture and displayed a dramatic red shift in the UV-vis spectrum.

Protasiewicz and co-workers reported a different approach toward the conjugated PPP polymers **40a–40d** using the so-called phospha-Wittig reaction (Scheme 4).[68,69] Polymer **40d** exhibited weak fluorescence with an emission maximum at *ca.* 540 nm, but a photoluminescence efficiency of only *ca.* 8% of that for *E*-stilbene. The weak fluorescence intensity *vs.* stilbene was attributed to quenching from the phosphorus lone pair, or a heavy atom effect. This research nevertheless demonstrated

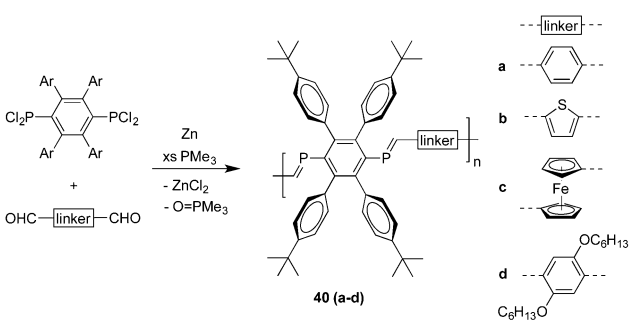

40 (a-d)

Scheme 4 Synthesis of **40** *via* phospha-Wittig reaction.

the emissive property of this class of PPP polymer materials for the first time. Later on, the same group also reported polymer **41** incorporating P=P linkages along the polymer backbone, but again with only weakly emissive features.

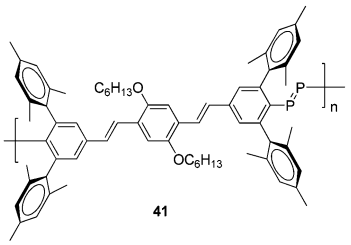

41

5. Silicon-containing polymers

Silicon-containing conjugated materials have been the subject of much recent interest for application in OLEDs, OPVs, and OFETs. Compared to their carbon analogues, these species have quite different electronic and optical properties, which arise from the σ*–π* interaction between the σ*-orbitals of the two exocyclic σ bonds and the π* orbital of the butadiene moiety, akin to the features observed in phospholes.[70] The unique interaction in these main group compounds leads to low-lying HOMO and LUMO energies and intriguing optoelectronic properties. One well-known example is poly(2,7-dibenzosilole) (**42**), reported by Holmes *et al.* as an excellent blue emitting polymer.[71] The HOMO and LUMO energy levels of **42** were determined to be −5.77 and −2.18 eV, respectively, which are about 0.1 eV lower than polyfluorene, its all-carbon congener. In addition, the incorporation of the Si atom leads to higher thermal stability and EL efficiency.

In general, silole and other conjugated fused relatives (*e.g.*, dibenzosilole, dithienosilole and ladder-type silaindacenodithiophene) are popular basic building blocks for the construction of conjugated polymers (Fig. 6). The incorporation of the silole moiety in conjugated polymers is of great interest and the materials have been well reviewed by Cao *et al.* in 2007.[72] More recently, conjugated siloles have attracted growing attention with regard to high-performance organic electronics, which will be the focus of this section. By fusing a central silole unit with two flanking thiophene or benzene rings, the systems were expected to combine the advantages of the intrinsic properties of silole with those of the cyclopentadithiophene or fluorene systems.

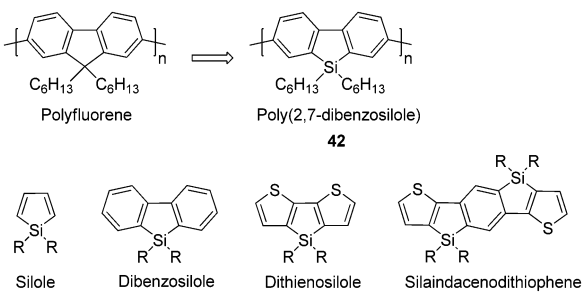

42

Fig. 6 Structures of silole building blocks.

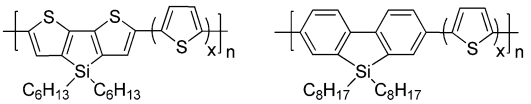

43a: x = 0 **44a**: x = 0
43b: x = 1 **44b**: x = 1
43c: x = 2 **44c**: x = 2

In 2008, a family of dithienosilole- and dibenzosilole-based thiophene copolymers, **43a–43c** and **44a–44c**, were investigated by Facchetti, Ratner, Marks and co-workers for application in OFETs.[73] Polymers **43a–43c** with the dithienosilole unit exhibit strong UV-vis absorption at λ_{max} = 521–544 nm, emit orange-red light in the range of λ_{max} = 601–620 nm, and possess small HOMO–LUMO energy gaps of 1.8–1.9 eV. Polymers **44a–44c** containing the dibenzosilole unit show a blue shift in both UV-vis absorption (377–503 nm) and emission (455–528 nm), in addition to relatively large energy gaps (2.3–2.9 eV). All of the polymers are thermally and environmentally stable. In terms of OFET performance, dithienosilole copolymers **43b** and **43c** exhibit hole mobilities as high as μ_h = 0.05 and μ_h = 0.08 $cm^2\ V^{-1}$ s, respectively. As a point of reference, it should be mentioned that mobilities higher than 10^{-3} $cm^2\ V^{-1}$ s are desirable for high-efficiency polymer solar cells in order to have efficient charge transport. This study demonstrated the valuable advantages of silole-containing polymers over their all-carbon counterparts in terms of better hole transport properties.

Another important application for conjugated silicon-containing polymers are organic solar cells. In 2008, Yang and co-workers reported the low band gap D–A polymer **45** (E_g = 1.45 eV) made up from alternating dithienosiloles as electron donor and benzothiadiazole units as electron acceptor.[74] The introduction of branched alkyl chains on the dithienosilole unit ensured improvement of the polymer propagation and its solubility. The polymer had a number-average molecular weight of M_n = 18 kDa and a polydispersity index of PDI = 1.2, as well as good thermal stability below 250 °C. Although the band gap of **45** is very similar to its C-analogue polymer, its hole mobility of $\mu_h = 3 \times 10^{-3}$ $cm^2\ V^{-1}$ s is about three times higher than that for the C-analogue, highlighting the benefits of the introduction of the Si atom. A bulk heterojunction (BHJ) photovoltaic device based on **45**/$PC_{71}BM$ (1 : 1, w/w) gave a PCE up to 5.1%, with J_{sc} 12.7 mA cm^{-2}, V_{oc} 0.68 V and FF 51.6%.

Apart from highlighting the intrinsic electronic merits of silole-containing polymers on the molecular orbitals and energies, the study by Yang and co-workers also showed that silicon-atom fusion enhances the solid state packing between polymer chains, which leads to improved charge transport.[75] The reason for this observation was attributed to the longer C–Si bond compared to the C–C bond that reduces the steric hindrance from the bulky alkyl groups, which was also confirmed by theoretical calculations.

Following this initial study that successfully applied a dithienosilole-containing polymer in a high-performance solar cell, a series of polymers with different alkyl substituted on dithienosilole moiety (**46a–46c**) were next developed by Yang and co-workers.[76] Polymers **46b** and **46c** with two branched 2-ethylhexyl or linear n-$C_{12}H_{25}$ alkyl chains showed good solubility in common organic solvents, however, **46a** with shorter alkyl chains could not be dissolved in common organic solvents. Both **46b** and **46c** showed strong absorption features in the range of λ_{max} = 400–800 nm. The band gaps calculated from the absorption edges (**46b**: 1.52 eV; **46c**: 1.53 eV) are slightly smaller than those calculated from electrochemistry (**46b**: 1.82 eV; **46c**: 1.83 eV), which was attributed to the interfacial barrier for charge injection. The hole-mobilities of **46b** and **46c** were measured to be $\mu_h = 3 \times 10^{-6}$ and $\mu_h = 3.6 \times 10^{-6}$ cm^{-2} V^{-1} s, respectively. In corresponding polymer/$PC_{71}BM$ devices (1 : 1; w/w), the performance of **46b** revealed a V_{oc} of 0.60 V, J_{sc} of 9.76 mA cm^{-2}, a FF of 50.3%, and a PCE of 2.95%. Under the same conditions, **46c** exhibited a slightly higher V_{oc} of 0.62 V, a higher J_{sc} of 10.67 mA cm^{-2}, and an equivalent FF of 51.8%, resulting in an efficiency of 3.43%. Overall, it was found that the side chains not only affect the solubility, but also the intermolecular packing, and consequently the device performance.

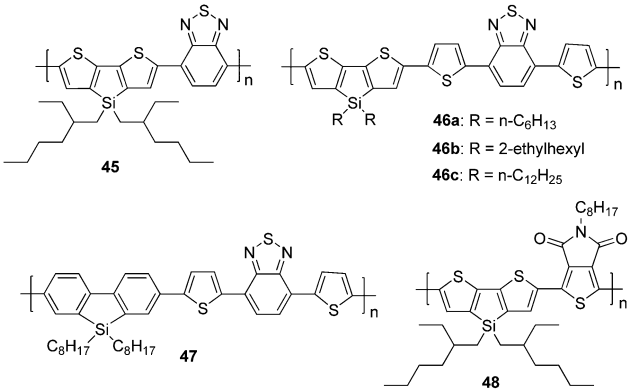

The structurally similar dibenzosilole-based polymer **47**, developed by Cao in 2008, also showed a high performance in an OPV device.[77] Compared to its carbon congener, the polymer exhibited a 0.1 eV lower optical band gap (1.82 eV) and a 20 nm red-shifted absorption maximum; the hole mobility of **47** was measured to be *ca.* $\mu_h = 1 \times 10^{-3}$ cm^2 V^{-1} s, which is almost 10 times higher than that of its carbon counterpart. By blending the polymer with $PC_{61}BM$, a PCE of up to 5.4% was achieved that was based on a V_{oc} of 0.90 V, a J_{sc} of 9.5 mA cm^{-2}, and a FF of 50.7%. It should be noted that an independent study using the same polymer was also reported by Leclerc and co-workers around the same time.[78]

In 2011, the D–A copolymer **48** consisting of alternating electron-accepting thieno[3,4-c]pyrrole-4,5-dione (TPD) and electron-donating dithienosilole was reported by Lu, Leclerc, Tao and co-workers.[79] Notably, the TPD unit has recently emerged as a very promising electron-deficient moiety, due to its rigidity, planar and good solubility. TPD-based polymers show very promising performance in OPVs with the PCEs as high as 8.5%, as summarized by Leclerc *et al.* very recently.[80] A film of polymer **48** showed strong absorption peaks at λ_{max} = 614 and 670 nm, with the onset absorption at λ_{onset} = 717 nm. It possesses a low band gap of E_g = 1.73 eV and a deep HOMO energy level (5.57 eV) that are important for increasing the J_{sc} and V_{oc} and consequently, the device performance. The hole mobility of the polymer was determined to be *ca.* $\mu_h = 1 \times 10^{-4}$ cm^2 V^{-1} s. By blending the polymer with $PC_{71}BM$ at a weight ratio of 1 : 2, the PV performance showed a high PCE of 7.3% with an active area of 1 cm^2, a V_{oc} of 0.88 V, a J_{sc} of 12.2 mA cm^{-2}, and a FF of 0.58. An OPV device with a thicker active layer (d > 200 nm) was also tested, with the PCE reaching 6.1%, indicating the promising potential for future fabrication by roll-to-roll printing techniques on a large area.

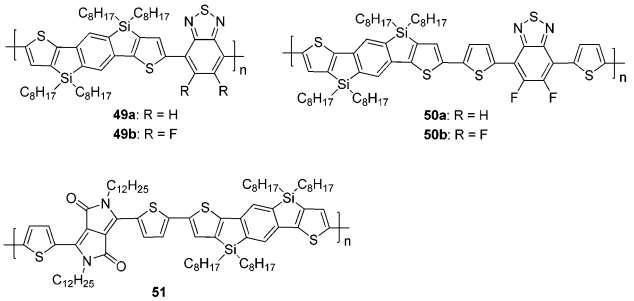

The ladder-type silaindacenodithiophene (SiIDT) with further extended π-conjugation is also attractive for the design of donor–acceptor copolymers. Besides the improved charge carrier mobilities, the incorporation of indacenodithiophene is also advantageous for improving the optical properties of the materials. It further reduces the conformation disorder, and facilitates beneficial intermolecular interactions. In 2011, Asharf and co-workers investigated the optoelectronic properties of polymer **49a**, consisting of the electron-donating SiIDT and the electron-accepting benzothiadiazole units.[81] The optical band gap derived from the absorption onset, and the HOMO energy from the ambient photo-electron spectroscopy (PESA) were determined to be E_g = −1.8 eV and E_{HOMO} = −5.5 eV, respectively. A BHJ device using polymer **49a**/$PC_{71}BM$ gave a higher PCE value of 4.3%, with a V_{oc} of 0.88 V, a J_{sc} of 0.99 mA cm^{-2} and a FF of 52%. It should be noted that independent work on the same polymer has also been reported by Jen and co-workers.[82]

Later on, the Asharf group developed polymers **49** and **50**, and investigated the effect of fluorine, and the thienyl spacer on the device performance.[83] Notably, the incorporation of fluorine atoms into conjugated polymers in general has recently attracted attention for application in high-efficiency photovoltaic devices.[84] Its electron-withdrawing character lowers the HOMO energy level, thereby increasing the V_{oc} and potentially improving the PCE. Moreover, due to its small size, it also causes no deleterious steric effect. In the case of polymers **49** and **50**, introduction of fluorine was found to lower both the HOMO and LUMO energy levels to the same degree (0.1 eV), without affecting the band gap. The

incorporation of the thienyl spacers in the polymer backbone, however, leads to significant improvement of the hole mobility (μ_h = 0.28 $cm^2\ V^{-1}\ s$ for **50a** and μ_h = 0.19 $cm^2\ V^{-1}\ s$ for **50b**), several orders of magnitude higher than those of **49a** and **49b**. The presence of fluorine in **50b** led to a higher PCE of 4.3%, compared to the 3.6% for its non-fluorinated counterpart.

By replacing the benzothiadiazole with DPP, polymer **51** exhibits high ambipolar charge transport abilities with a hole mobility of μ_h = 0.65 $cm^2\ V^{-1}\ s$ and an electron mobility of μ_e = 0.1 $cm^2\ V^{-1}\ s$.

6. Germanium-containing polymers

Germanium, like carbon and silicon, belongs to group 14, which shows a dramatic increase in the metallic character upon going from carbon (a non-metal) to lead (a metal); the metalloid germanium (Ge) sits below the semimetal silicon, whose intrinsic properties already lead to considerably distinct features from those of all-carbon based optoelectronic materials. As mentioned in the previous section, replacement of carbon with silicon leads to lower band gaps, improved charge transport, better intermolecular packing, and therefore, enhanced performance in organic solar cells. Along the same lines, introduction of Ge was expected to exhibit a similar, if not more pronounced, effect on the optical properties and molecular ordering. The longer Ge–C bond (1.96 Å) relative to the Si–C bond (1.88 Å),[85] would further remove the bulky side chains from the conjugated polymer chains, allowing for even stronger π-stacking interactions. In addition, the higher electronegativity of Ge (χ = 2.01) relative to Si (χ = 1.90), may reduce the polarization of the C–Ge bond and render arylgermanes much more stable. This was experimentally confirmed by Heeney and co-workers by means of the dithienogermole system that is sufficiently stable under basic conditions to undergo Suzuki polycondensation, unlike its dithienosilole analogue.[85]

In 2010, Leclerc and co-workers reported the synthesis of germafluorene, and the series of conjugated homopolymers and copolymers **52–54** based on it, as well as their application in field-effect transistors and bulk heterojunction solar cells.[86] Similar to polyfluorene and poly(2,7-dibenzosilole), poly(germafluorene) **52** displays a strong blue emission with a quantum yield of ϕ_{PL} = 0.54. For **53**, two strong absorption bands at λ_{max} = 375 and 688 nm were observed, with the optical band gap measured to be E_g = 1.63 eV. Its best performance in FETs revealed a hole mobility up to μ_h = 0.04 $cm^2\ V^{-1}\ s$ and an I_{on}/I_{off} ratio of 1.0 × 10^6. The absorption of **54** displayed two bands at λ_{max} = 403 and 580 nm, with the onset at λ_{onset} = 693 nm. The optical band gap is 1.79 eV, which is lower than fluorene (1.90 eV)[87] and its dibenzosilole analogue (1.85 eV),[78] probably due to the better intermolecular packing. In combination with $PC_{71}BM$, **54** shows a J_{sc} of 6.9 mA cm^{-2}, a FF of 0.51, a V_{oc} of 0.79 V, and a PCE of 2.8%.

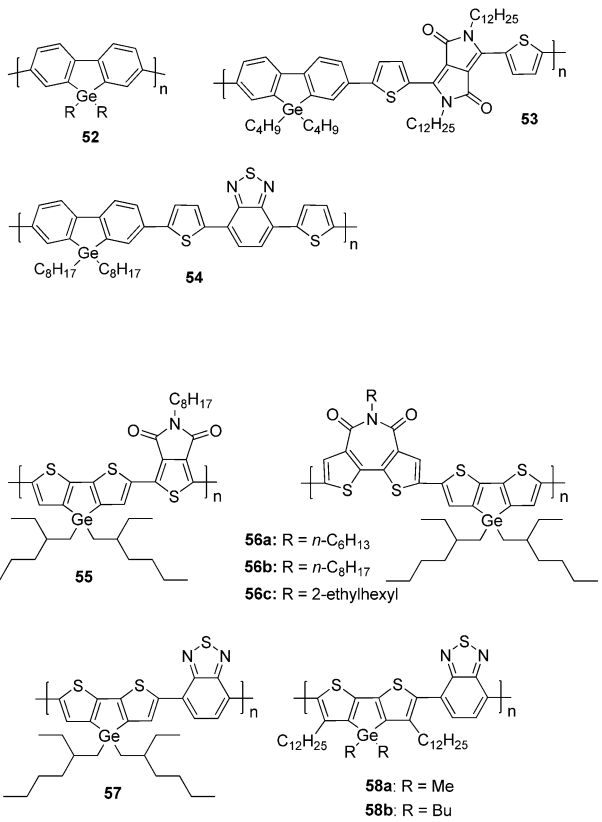

In 2011, Reynolds and co-workers reported a high bulk heterojunction photovoltaic performance for the first dithienogermole-containing conjugated polymer (**55**);[88] its silicon-based congener had already been demonstrated to show high performance in BHJs before. The optimized geometries of dithienosilole (left) and dithienogermole (right) monomers with methyl substituents reveal longer Ge–C bonds that alleviate the steric stress of the methyl groups and thus allow for stronger π–π stacking (Fig. 7). Upon substitution of the silicon atom for germanium, a red-shifted absorption spectrum (λ_{max} = 618 and 679 nm) was observed, along with a smaller band gap of 1.69 eV (*cf.*: 1.73 eV for the Si analogue). The lower band gap of the Ge-based polymer is due to the increase in the HOMO energy, while the LUMO energy remains identical with its Si analogue. BHJ solar cells were fabricated using an inverted architecture, ITO/ZnO/Polymer:$PC_{71}BM$/MoO_3/Ag, which is advantageous in avoiding rapid oxidation

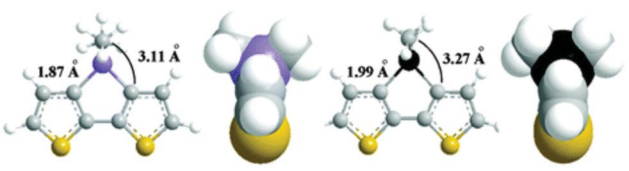

Fig. 7 MM2 optimized geometries of dimethyl-substituted dithienosilole (left) and dithienogermole (right) heterocycles, showing C–X bond lengths and distances of methyl groups from the nearest thienyl carbon. Adapted with permission from ref. 88. Copyright 2011 American Chemical Society.

of low work-function metal cathodes and etching of the ITO by the acid. After optimization, polymer **55** gave a high PCE value of 7.3%, with a J_{sc} of 12.6 mA cm^{-2}, FF of 68%, and a V_{oc} of 0.85 V. Under the same conditions, the Si-containing polymer only gave a PCE of 6.6%, with a J_{sc} of 11.5 mA cm^{-2}, FF of 65%, and a V_{oc} of 0.89 V. The enhanced performance of the Ge-species is the result of a higher short-circuit current and fill factor in the dithienogermole-containing polymer, at the slight cost of a lower open circuit voltage due to the higher HOMO energy level.

Very recently, the series of D–A copolymers **56a–56c** with alternating electron-donating dithienogermole and electron-accepting bithiophene imide (BTI) has been developed by the groups of Ratner, Chang, Facchetti, and Marks.[89] The electron-acceptor BTI was utilized for constructing homopolymers and various D–A copolymers in high-performance FETs and solar cells. Inverted BHJ solar cells that blended the polymer with $PC_{71}BM$ showed promising device performance with PCE values of 3.62–4.77%.

By replacing the electron-accepting BTI units with benzothiadiazole, Heeney and co-workers reported the D–A copolymer **57**, and its application in transistors and photovoltaic solar cells.[85] This polymer showed a small optical band gap of 1.47 eV, and high charge carrier mobility of 0.11 cm^2 V^{-1} s. A photovoltaic device based on this polymer and $PC_{71}BM$ exhibited a PCE of 4.5% with a high J_{sc} of 18.6 mA cm^{-2}. Almost at the same time, independent work using the same polymer has also been carried out by the groups of Leclerc and Ohshita.[90,91] Further modification of this system (**58**) by changing the peripheral alkyl chains and comparing these species with the dithienosilole analogues was carried out by Heeney, Kim and their co-workers,[92] and upon going from Si to Ge, enhanced charge mobility was observed. In addition, shortening the side chain from butyl to methyl was found to also lead to a smooth device morphology and better performance (PCE: 2.66%).

7. Boron-containing polymers

Boron-containing π-conjugated materials have attracted increased attention because of their unique properties stemming from the p–π* conjugation between the vacant p orbital on the boron atom with the π* orbital of the π-conjugated framework. This class of materials with unique photophysical properties has found a variety of optoelectronic applications, particularly in OLEDs and fluorescent sensors.[93–95] The topic of organoborane polymers for the optical, electronic and sensory applications has recently been excellently reviewed by Jäkle[93] and will therefore be presented only very briefly as part of this review to provide the reader with a general overview of these polymers. Structurally, the boron center can be embedded into the main chain of conjugated polymers, or appended in side chains of conjugated polymers (Fig. 8). In terms of coordination number, the organoborane moieties can be classified as tricoordinate and tetracoordinate. Extensive

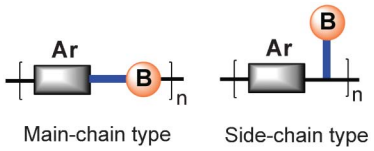

Fig. 8 Main-chain type and side-chain type conjugated organoborane polymers.

efforts in this area have created a variety of synthetic protocols toward boron-containing conjugated polymers. The synthetic methods for tricoordinate organoborane polymers are summarized in Scheme 5.

The hydroboration[96–99] and haloboration-phenylboration[100] polymerization synthetic protocols were first explored by Chujo and co-workers, and have been shown as the most versatile synthetic methods for the incorporation of tricoordinate boron species into the main chain of conjugated polymers. Recently, the hydroboration method has also been applied for the development of an interesting class of polymer (**60a** and **60b**), starting from a polymeric diboraanthracene **59** (Scheme 6).[101] The rigid and planar diboraanthracene unit has the advantage in maximizing the π-conjugation through the empty p orbital at boron. The long alkyl chains in **60b** greatly improve the solubility. Optical spectroscopy revealed absorption maxima for **60a** and **60b** at λ_{max} = 384 and 410 nm, respectively. The red shift of the absorption of **60b** was attributed to the presence of the electron-donating alkoxy

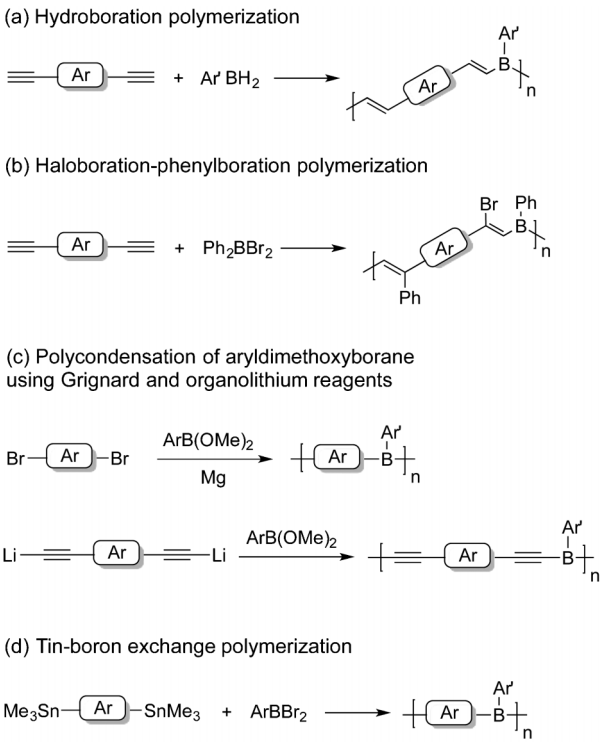

Scheme 5 Summary of the synthetic methods toward tricoordinate organoborane polymers.

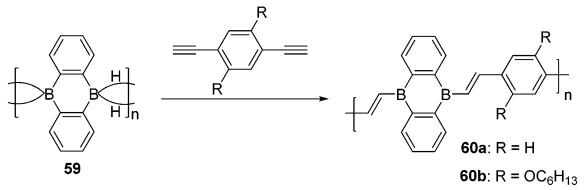

Scheme 6 Synthesis of **60** using hydroboration polymerization.

group, supporting the electron-accepting character of the organoboron framework. Polymer **60b** showed a distinct green emission both in solution and the solid state. The emission maximum and quantum yield of **60b** in toluene were measured to be λ_{em} = 518 nm and ϕ_{PL} = 0.09, respectively. A slightly red-shifted emission was observed with increasing solvent polarity, suggesting the significant polarization of the excited state.

Chujo and co-workers also developed a polymerization procedure for preparing the conjugated organoboron polymers **61** and **62** (Scheme 5b).[102,103] Polymers **61** show absorption maxima in the range of λ_{max} = 359–367 nm in $CHCl_3$ solution and emit blue-green light (λ_{em} = 477–496 nm) upon excitation at 350 nm. Polymer **62** exhibits absorption at λ_{em} = 397 nm, and blue emission.

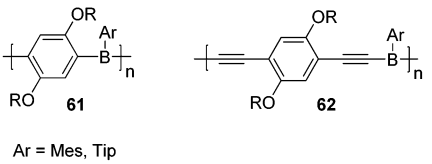

Tin-boron exchange polymerization, first introduced by Jäkle and co-workers in 2005, is a highly selective polymerization method under very mild conditions (Scheme 7).[104] Polymers **63a–63c** were reported to exhibit intriguing photophysical properties, which were found to be highly dependent on the choice of the pendant aryl substituent. Polymers **63a** and **63b** are highly emissive with quantum yields in CH_2Cl_2 solution determined to be ϕ_{PL} = 0.21 and ϕ_{PL} = 0.15, respectively. Compared to **63a**, attachment of the electron-accepting C_6F_5 pendant group in **63b** leads to red shifts in both the UV-vis absorption (from 391 to 413 nm) and the emission (from 491 to 529 nm) wavelengths. Compared with

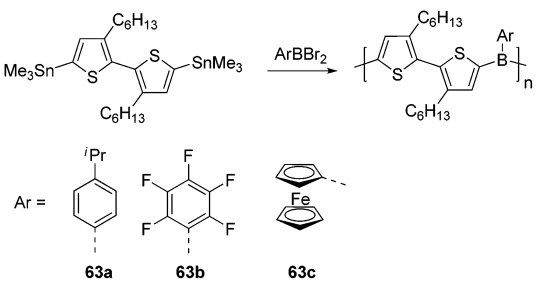

Scheme 7 Synthesis of organoboron polymers **63** *via* tin-boron exchange.

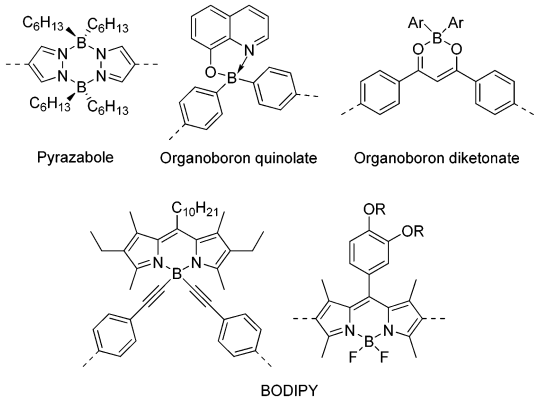

Fig. 9 Examples of tetracoordinate organoboron units for the construction of polymers.

their model compounds, polymers **63a** and **63b** revealed a red shift of the solution absorption, indicative of a considerable degree of extended p–π conjugation within the polymer main chain; polymer **63c** is deep dark red-colored, but not emissive. In addition, these polymers showed an interesting sensing property toward pyridine by binding to the highly Lewis acidic boron sites.

In contrast to the tricoordinate species, introduction of the organoborane moieties with coordination number four into the conjugated polymers provides highly stable materials. Pyrazabole,[105] organoboron diketonate,[106] BODIPY[107–109] and organoboron quinolate,[110–112] are commonly used tetracoordinate organoboron units for the construction of polymers (Fig. 9). The last three building blocks are important, highly emissive materials, which have found widespread applications in OLEDs and fluorescent sensors. Their incorporation in polymers would thus lead to processable materials with very promising photophysical properties. It should be mentioned that, due to the tetrahedral geometry of the boron center involving all available B-orbitals, the p orbital is basically unavailable for electronic delocalization. General synthetic methods towards these types of polymers are commonly Pd-catalyzed cross-coupling reactions, such as Sonagashira or Suzuki coupling.

Taking organoboron quinolate as example, not only is this moiety is highly emissive, but also it also provides various methods for incorporating this chromophore into conjugated polymers. The earliest examples of main-chain organoboron quinolate polymers (**64**) were reported by Chujo and co-

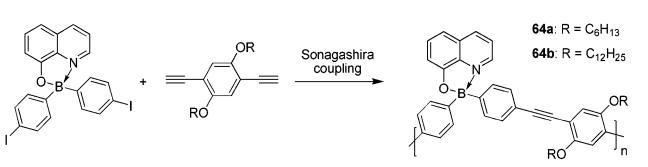

Scheme 8 Synthesis of main-chain organoboron quinolate polymers **64** *via* Sonagashira coupling.

workers in 2007;[110] the polymers were synthesized *via* Sonagashira–Hagaihara coupling reaction (Scheme 8). Polymer **64b** with longer alkyl chains showed improved solubility and thus larger molecular weights. However, both polymers showed very similar optical features. Compared to the iodo-monomer, a dramatic red shift in the UV-vis absorption was observed for the polymers, supporting extended π-conjugation along the polymer chain. The polymers also showed intense blue-green photoluminescence with emission wavelengths in solution and as thin films in the range of λ_{em} = 485–512 nm, and solution quantum yields of ϕ_{PL} = 0.26–0.27.

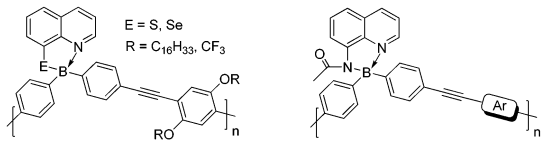

Chujo and co-workers also studied the single atom effect *via* changing the heteroatoms (E) in polymers **65** from O to the heavier Group 16 elements S and Se;[111] increasing the atomic number leads to a strong red shift in the emission and decreased photoluminescence efficiency. DFT calculations on molecular model systems have revealed a decreasing HOMO–LUMO gap upon incorporating S and Se, which was consistent with the bathochromic shift of the emission. Another series of organoboron aminoquinolate polymers **66**, developed by the same group, exhibited intense green photoluminescence and showed an efficient energy transfer from the conjugated linkers to the aminoquinolate units.[112]

In 2009, Jäkle and co-workers introduced a novel post-modification of bromoborane polymer precursor **67** to incorporate the organoboron quinolate moiety into the polymer chain (Scheme 9).[113] Reaction of the precursor polymer with 8-methoxyquinoline derivatives led to instant methyl deprotection and boron coordination, with rapid color change to bright-yellow or orange-red for **68a** and **68b**, respectively. Polymers **68a** and **68b** are highly stable and readily soluble in common organic solvents. The π-conjugation through the tetracoordinate boron centers was again found to be poor due to the unavailability of a suitable p orbital at boron. However, the polymer main chain acts as an ''antenna'' for the quinolato chromophore, similar to polymer **64** reported by Chujo and co-workers. Polymers **68a** and **68b** emit green (ϕ_{PL} = 0.21) and red light (ϕ_{PL} = 0.01) with moderate/weak efficiencies, respectively. Polymer **68a** has also been demonstrated to be selective sensor towards F^- and CN^- *via* large UV-vis and emission spectra changes upon binding of the analyte.

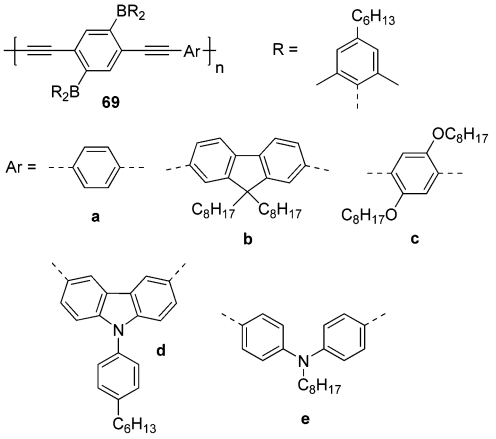

Apart from the extensively studied main-chain type boron-containing conjugated polymers, polymers with borane groups in the side chain are another important class of materials, albeit less explored. Yamaguchi and co-workers reported a series of poly-(aryleneethynylene)s **69** containing diarylboryl pendant groups.[114] All of the polymers exhibit intense emission in both solution and the solid state, with remarkable quantum yields of ϕ_{PL} = 0.87–0.98 (in benzene) and ϕ_{PL} = 0.36–0.54 (in the solid). On going from solution to a thin film, no obvious change was observed either in the absorption, or fluorescence spectra. Moreover, the fluorescence properties of these polymers can be easily tuned by the choice of the co-monomer units. With an increase in the electron-donating ability of the co-monomer units, the emission maxima of the films gradually shifted to longer wavelengths from λ_{em} = 489 (**69a**), to λ_{em} = 504 nm (**69b**), to λ_{em} = 527 nm (**69c**), to λ_{em} = 529 nm (**69d**), and to λ_{em} = 567 nm (**69e**).

In a related study, Jäkle and his group reported the organoborane-substituted polythiophene **71** that was accessible *via* side group borylation of the silylated polymer **70**.[115] The borylated polymer **71** displayed a distinct bathochromic shift in both absorption (*ca.* 60 nm) and emission (*ca.* 63 nm) relative to that of **70** (Fig. 10), demonstrating a narrowed energy band gap due to the presence of electron-withdrawing

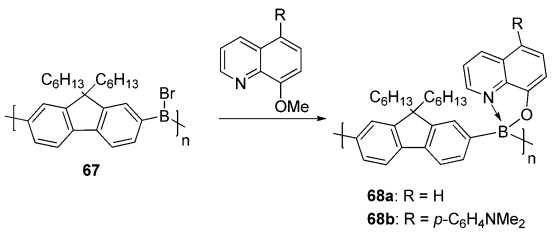

Scheme 9 Synthesis of **68** by postmodification of bromoborane precursor polymer **67**.

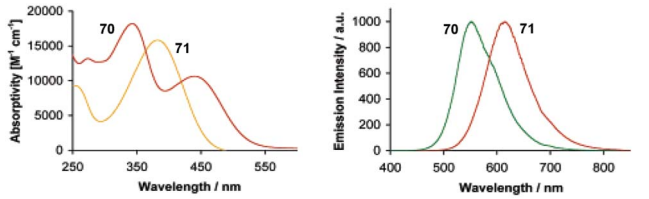

Fig. 10 UV-Vis absorption and emission spectra of PT-$SiMe_3$ (**70**) and PT-$BMes_2$ (**71**) in CH_2Cl_2 solution. Adapted with permission from ref. 115.

boryl side groups. The strongly electron-accepting features of **71** were confirmed by cyclic voltammetry, where the reduction potential of **71** is considerably less cathodic than those of silylated polymer **70**. This research offered a new efficient synthetic strategy to access borylated polythiophene and also opened up opportunities for the area of sensor materials.

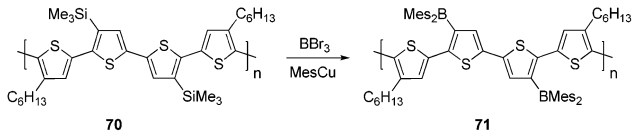

70 **71**

8. Conclusions

In conclusion, the incorporation of main-group elements into conjugated polymers is a powerful tool to endow the materials with distinct optoelectronic properties. While still at the proof-of-concept stage for many materials, researchers have been able to uncover promising applications within the field of optoelectronics in several instances. Some of the areas, *e.g.*, B- and Si-containing conjugated polymers, have experienced tremendous growth during the last decade, while others, *e.g.*, P- and Se-based materials, are quickly picking up steam due to the impressive features that have now been established for many main-group elements. A variety of new synthetic methods and different types of polymers have been reported. Other fields (*e.g.* Ge- and Te-containing polymers) are still in their infancy; however, they have clearly proven their promising potential for application in OPVs. Overall, due to the unique physical and chemical properties of the main-group elements, the field of main-group containing conjugated polymers can be anticipated to attract increasing attention and continues to play an important role for application in optoelectronic devices in the future.

Acknowledgements

Financial support by NSERC of Canada, and the Canada School for Energy and Environment is gratefully acknowledged.

Notes and references

1 T. A. Skotheim, R. L. Elsenbaumer and J. R. Reynolds, *Handbook of Conducting Polymers*, 2nd edn, revised and expanded, Marcel Dekker, Inc., New York, 1997.
2 *Design and Synthesis of Conjugated Polymers*, ed. M. Leclerc and J.-F. Morin, Wiley-VCH Verlag GmbH & Co. KGaA, 2010.
3 Y. Chujo, in *Conjugated Polymer Synthesis*, Wiley-VCH Verlag GmbH & Co. KGaA, 2010.
4 Y.-J. Cheng, S.-H. Yang and C.-S. Hsu, *Chem. Rev.*, 2009, **109**, 5868–5923.
5 J. Chen and Y. Cao, *Acc. Chem. Res.*, 2009, **42**, 1709–1718.
6 H. J. Son, F. He, B. Carsten and L. Yu, *J. Mater. Chem.*, 2011, **21**, 18934–18945.
7 P. L. Burn, S. C. Lo and I. D. W. Samuel, *Adv. Mater.*, 2007, **19**, 1675–1688.
8 A. Facchetti, *Chem. Mater.*, 2010, **23**, 733–758.
9 Z. Bao and J. Locklin, in *Organic Field Effect Transistors*, Taylor & Francis Group, LLC, 2007.
10 M. C. Scharber, D. Mühlbacher, M. Koppe, P. Denk, C. Waldauf, A. J. Heeger and C. J. Brabec, *Adv. Mater.*, 2006, **18**, 789–794.
11 I. F. Perepichka and D. F. Perepichka, *Handbook of Thiophene-Based Materials: Applications in Organic Electronics and Photonics*, John Wiley & Sons, Ltd, 2009.
12 I. Osaka and R. D. McCullough, *Acc. Chem. Res.*, 2008, **41**, 1202–1214.
13 C. J. Brabec, S. Gowrisanker, J. J. M. Halls, D. Laird, S. Jia and S. P. Williams, *Adv. Mater.*, 2010, **22**, 3839–3856.
14 M. Heeney, W. Zhang, D. J. Crouch, M. L. Chabinyc, S. Gordeyev, R. Hamilton, S. J. Higgins, I. McCulloch, P. J. Skabara, D. Sparrowe and S. Tierney, *Chem. Commun.*, 2007, 5061–5063.
15 A. M. Ballantyne, L. Chen, J. Nelson, D. D. C. Bradley, Y. Astuti, A. Maurano, C. G. Shuttle, J. R. Durrant, M. Heeney, W. Duffy and I. McCulloch, *Adv. Mater.*, 2007, **19**, 4544–4547.
16 Z. Chen, H. Lemke, S. Albert-Seifried, M. Caironi, M. M. Nielsen, M. Heeney, W. Zhang, I. McCulloch and H. Sirringhaus, *Adv. Mater.*, 2010, **22**, 2371–2375.
17 A. Patra, Y. H. Wijsboom, S. S. Zade, M. Li, Y. Sheynin, G. Leitus and M. Bendikov, *J. Am. Chem. Soc.*, 2008, **130**, 6734–6736.
18 M. Li, A. Patra, Y. Sheynin and M. Bendikov, *Adv. Mater.*, 2009, **21**, 1707–1711.
19 M. Li, Y. Sheynin, A. Patra and M. Bendikov, *Chem. Mater.*, 2009, **21**, 2482–2488.
20 Y. H. Wijsboom, A. Patra, S. S. Zade, Y. Sheynin, M. Li, L. J. W. Shimon and M. Bendikov, *Angew. Chem., Int. Ed.*, 2009, **48**, 5443–5447.
21 A. Patra and M. Bendikov, *J. Mater. Chem.*, 2010, **20**, 422–433.
22 O. Gidron, Y. Diskin-Posner and M. Bendikov, *J. Am. Chem. Soc.*, 2010, **132**, 2148–2150.
23 H. Kong, D. S. Chung, I.-N. Kang, J.-H. Park, M.-J. Park, I. H. Jung, C. E. Park and H.-K. Shim, *J. Mater. Chem.*, 2009, **19**, 3490–3499.
24 A. J. Kronemeijer, E. Gili, M. Shahid, J. Rivnay, A. Salleo, M. Heeney and H. Sirringhaus, *Adv. Mater.*, 2012, **24**, 1558–1565.
25 M. Shahid, R. S. Ashraf, Z. Huang, A. J. Kronemeijer, T. McCarthy-Ward, I. McCulloch, J. R. Durrant, H. Sirringhaus and M. Heeney, *J. Mater. Chem.*, 2012, **22**, 12817–12823.
26 M. Shahid, T. McCarthy-Ward, J. Labram, S. Rossbauer, E. B. Domingo, S. E. Watkins, N. Stingelin, T. D. Anthopoulos and M. Heeney, *Chem. Sci.*, 2012, **3**, 181–185.
27 L. Bürgi, M. Turbiez, R. Pfeiffer, F. Bienewald, H.-J. Kirner and C. Winnewisser, *Adv. Mater.*, 2008, **20**, 2217–2224.
28 J. C. Bijleveld, A. P. Zoombelt, S. G. J. Mathijssen, M. M. Wienk, M. Turbiez, D. M. de Leeuw and R. A. J. Janssen, *J. Am. Chem. Soc.*, 2009, **131**, 16616–16617.

29 J. Lee, A. R. Han, J. Kim, Y. Kim, J. H. Oh and C. Yang, *J. Am. Chem. Soc.*, 2012, **134**, 20713–20721.
30 L. Dou, W.-H. Chang, J. Gao, C.-C. Chen, J. You and Y. Yang, *Adv. Mater.*, 2013, **25**, 825–831.
31 J. Hollinger, A. Jahnke, N. Coombs and D. S. Seferos, *J. Am. Chem. Soc.*, 2010, **132**, 8546–8547.
32 A. A. Jahnke and D. S. Seferos, *Macromol. Rapid Commun.*, 2011, **32**, 943–951.
33 A. Patra, Y. H. Wijsboom, G. Leitus and M. Bendikov, *Org. Lett.*, 2009, **11**, 1487–1490.
34 A. A. Jahnke, G. W. Howe and D. S. Seferos, *Angew. Chem., Int. Ed.*, 2010, **49**, 10140–10144.
35 G. L. Gibson, T. M. McCormick and D. S. Seferos, *J. Am. Chem. Soc.*, 2011, **134**, 539–547.
36 A. A. Jahnke, B. Djukic, T. M. McCormick, E. Buchaca Domingo, C. Hellmann, Y. Lee and D. S. Seferos, *J. Am. Chem. Soc.*, 2013, **135**, 951–954.
37 T. Baumgartner and R. Réau, *Chem. Rev.*, 2006, **106**, 4681–4727.
38 M. Hissler, P. W. Dyer and R. Reau, *Top. Curr. Chem.*, 2005, **250**, 127–163.
39 M. Hissler, P. W. Dyer and R. Réau, *Coord. Chem. Rev.*, 2003, **244**, 1–44.
40 D. P. Gates, *Top. Curr. Chem.*, 2005, **250**, 107–126.
41 Y. Ren and T. Baumgartner, *Dalton Trans.*, 2012, **41**, 7792–7800.
42 Y. Matano and H. Imahori, *Org. Biomol. Chem.*, 2009, **7**, 1258–1271.
43 A. Fukazawa, M. Hara, T. Okamoto, E.-C. Son, C. Xu, K. Tamao and S. Yamaguchi, *Org. Lett.*, 2008, **10**, 913–916.
44 A. Saito, T. Miyajima, M. Nakashima, T. Fukushima, H. Kaji, Y. Matano and H. Imahori, *Chem.–Eur. J.*, 2009, **15**, 10000–10004.
45 Y. Matano, A. Saito, T. Fukushima, Y. Tokudome, F. Suzuki, D. Sakamaki, H. Kaji, A. Ito, K. Tanaka and H. Imahori, *Angew. Chem., Int. Ed.*, 2011, **50**, 8016–8020.
46 E. Deschamps, L. Ricard and F. Mathey, *Angew. Chem., Int. Ed. Engl.*, 1994, **33**, 1158–1161.
47 A. Saito, Y. Matano and H. Imahori, *Org. Lett.*, 2010, **12**, 2675–2677.
48 S. S. H. Mao and T. D. Tilley, *Macromolecules*, 1997, **30**, 5566–5569.
49 C. Hay, C. Fischmeister, M. Hissler, L. Toupet and R. Réau, *Angew. Chem., Int. Ed.*, 2000, **39**, 1812–1815.
50 C. Hay, M. Hissler, C. Fischmeister, J. Rault-Berthelot, L. Toupet, L. Nyulászi and R. Réau, *Chem.–Eur. J.*, 2001, **7**, 4222–4236.
51 M. Sebastian, M. Hissler, C. Fave, J. Rault-Berthelot, C. Odin and R. Réau, *Angew. Chem., Int. Ed.*, 2006, **45**, 6152–6155.
52 V. Lemau de Talance, M. Hissler, L.-Z. Zhang, T. Karpati, L. Nyulaszi, D. Caras-Quintero, P. Bauerle and R. Reau, *Chem. Commun.*, 2008, 2200–2202.
53 H.-S. Na, Y. Morisaki, Y. Aiki and Y. Chujo, *Polym. Bull.*, 2007, **58**, 645–652.
54 Y. Morisaki, H.-S. Na, Y. Aiki and Y. Chujo, *Polym. Bull.*, 2007, **58**, 777–784.
55 H.-S. Na, Y. Morisaki, Y. Aiki and Y. Chujo, *J. Polym. Sci., Part A: Polym. Chem.*, 2007, **45**, 2867–2875.
56 T. Baumgartner, T. Neumann and B. Wirges, *Angew. Chem., Int. Ed.*, 2004, **43**, 6197–6201.
57 T. Baumgartner, W. Bergmans, T. Kárpáti, T. Neumann, M. Nieger and L. Nyulászi, *Chem.–Eur. J.*, 2005, **11**, 4687–4699.
58 Y. Dienes, S. Durben, T. Kárpáti, T. Neumann, U. Englert, L. Nyulászi and T. Baumgartner, *Chem.–Eur. J.*, 2007, **13**, 7487–7500.
59 Y. Ren, W. H. Kan, M. A. Henderson, P. G. Bomben, C. P. Berlinguette, V. Thangadurai and T. Baumgartner, *J. Am. Chem. Soc.*, 2011, **133**, 17014–17026.
60 Y. Ren, W. H. Kan, V. Thangadurai and T. Baumgartner, *Angew. Chem., Int. Ed.*, 2012, **51**, 3964–3968.
61 C. Romero-Nieto, S. Durben, I. M. Kormos and T. Baumgartner, *Adv. Funct. Mater.*, 2009, **19**, 3625–3631.
62 S. Durben, D. Nickel, R. A. Krüger, T. C. Sutherland and T. Baumgartner, *J. Polym. Sci., Part A: Polym. Chem.*, 2008, **46**, 8179–8190.
63 R. A. Krüger, T. J. Gordon, T. C. Sutherland and T. Baumgartner, *J. Polym. Sci., Part A: Polym. Chem.*, 2011, **49**, 1201–1209.
64 S. Durben, Y. Dienes and T. Baumgartner, *Org. Lett.*, 2006, **8**, 5893–5896.
65 R.-F. Chen, R. Zhu, Q.-L. Fan and W. Huang, *Org. Lett.*, 2008, **10**, 2913–2916.
66 V. A. Wright and D. P. Gates, *Angew. Chem., Int. Ed.*, 2002, **41**, 2389–2392.
67 V. A. Wright, B. O. Patrick, C. Schneider and D. P. Gates, *J. Am. Chem. Soc.*, 2006, **128**, 8836–8844.
68 R. C. Smith, X. Chen and J. D. Protasiewicz, *Inorg. Chem.*, 2003, **42**, 5468–5470.
69 R. C. Smith and J. D. Protasiewicz, *J. Am. Chem. Soc.*, 2004, **126**, 2268–2269.
70 S. Yamaguchi and K. Tamao, *J. Chem. Soc., Dalton Trans.*, 1998, 3693–3702.
71 K. L. Chan, M. J. McKiernan, C. R. Towns and A. B. Holmes, *J. Am. Chem. Soc.*, 2005, **127**, 7662–7663.
72 J. Chen and Y. Cao, *Macromol. Rapid Commun.*, 2007, **28**, 1714–1742.
73 G. Lu, H. Usta, C. Risko, L. Wang, A. Facchetti, M. A. Ratner and T. J. Marks, *J. Am. Chem. Soc.*, 2008, **130**, 7670–7685.
74 J. Hou, H.-Y. Chen, S. Zhang, G. Li and Y. Yang, *J. Am. Chem. Soc.*, 2008, **130**, 16144–16145.
75 H.-Y. Chen, J. Hou, A. E. Hayden, H. Yang, K. N. Houk and Y. Yang, *Adv. Mater.*, 2010, **22**, 371–375.
76 L. Huo, H.-Y. Chen, J. Hou, T. L. Chen and Y. Yang, *Chem. Commun.*, 2009, 5570–5572.
77 E. Wang, L. Wang, L. Lan, C. Luo, W. Zhuang, J. Peng and Y. Cao, *Appl. Phys. Lett.*, 2008, **92**, 033307.
78 P.-L. T. Boudreault, A. Michaud and M. Leclerc, *Macromol. Rapid Commun.*, 2007, **28**, 2176–2179.
79 T.-Y. Chu, J. Lu, S. Beaupré, Y. Zhang, J.-R. M. Pouliot, S. Wakim, J. Zhou, M. Leclerc, Z. Li, J. Ding and Y. Tao, *J. Am. Chem. Soc.*, 2011, **133**, 4250–4253.
80 A. Pron, P. Berrouard and M. Leclerc, *Macromol. Chem. Phys.*, 2013, **214**, 7–16.
81 R. S. Ashraf, Z. Chen, D. S. Leem, H. Bronstein, W. Zhang, B. Schroeder, Y. Geerts, J. Smith, S. Watkins, T. D. Anthopoulos, H. Sirringhaus, J. C. de Mello, M. Heeney and I. McCulloch, *Chem. Mater.*, 2010, **23**, 768–770.

82 J.-Y. Wang, S. K. Hau, H.-L. Yip, J. A. Davies, K.-S. Chen, Y. Zhang, Y. Sun and A. K. Y. Jen, *Chem. Mater.*, 2010, **23**, 765–767.
83 B. C. Schroeder, Z. Huang, R. S. Ashraf, J. Smith, P. D'Angelo, S. E. Watkins, T. D. Anthopoulos, J. R. Durrant and I. McCulloch, *Adv. Funct. Mater.*, 2012, **22**, 1663–1670.
84 S. C. Price, A. C. Stuart, L. Yang, H. Zhou and W. You, *J. Am. Chem. Soc.*, 2011, **133**, 4625–4631.
85 Z. Fei, J. S. Kim, J. Smith, E. B. Domingo, T. D. Anthopoulos, N. Stingelin, S. E. Watkins, J.-S. Kim and M. Heeney, *J. Mater. Chem.*, 2011, **21**, 16257–16263.
86 N. Allard, R. D. B. Aïch, D. Gendron, P.-L. T. Boudreault, C. Tessier, S. Alem, S.-C. Tse, Y. Tao and M. Leclerc, *Macromolecules*, 2010, **43**, 2328–2333.
87 Q. Zhou, Q. Hou, L. Zheng, X. Deng, G. Yu and Y. Cao, *Appl. Phys. Lett.*, 2004, **84**, 1653.
88 C. M. Amb, S. Chen, K. R. Graham, J. Subbiah, C. E. Small, F. So and J. R. Reynolds, *J. Am. Chem. Soc.*, 2011, **133**, 10062–10065.
89 X. Guo, N. Zhou, S. J. Lou, J. W. Hennek, R. Ponce Ortiz, M. R. Butler, P.-L. T. Boudreault, J. Strzalka, P.-O. Morin, M. Leclerc, J. T. López Navarrete, M. A. Ratner, L. X. Chen, R. P. H. Chang, A. Facchetti and T. J. Marks, *J. Am. Chem. Soc.*, 2012, **134**, 18427–18439.
90 D. Gendron, P.-O. Morin, P. Berrouard, N. Allard, B. R. Aïch, C. N. Garon, Y. Tao and M. Leclerc, *Macromolecules*, 2011, **44**, 7188–7193.
91 J. Ohshita, Y.-M. Hwang, T. Mizumo, H. Yoshida, Y. Ooyama, Y. Harima and Y. Kunugi, *Organometallics*, 2011, **30**, 3233–3236.
92 J. S. Kim, Z. Fei, D. T. James, M. Heeney and J.-S. Kim, *J. Mater. Chem.*, 2012, **22**, 9975–9982.
93 F. Jäkle, *Chem. Rev.*, 2010, **110**, 3985–4022.
94 Z. M. Hudson and S. Wang, *Acc. Chem. Res.*, 2009, **42**, 1584–1596.
95 C. R. Wade, A. E. J. Broomsgrove, S. Aldridge and F. O. P. Gabbaï, *Chem. Rev.*, 2010, **110**, 3958–3984.
96 N. Matsumi, K. Naka and Y. Chujo, *J. Am. Chem. Soc.*, 1998, **120**, 5112–5113.
97 N. Matsumi, M. Miyata and Y. Chujo, *Macromolecules*, 1999, **32**, 4467–4469.
98 N. Matsumi, Y. Chujo, O. Lavastre and P. H. Dixneuf, *Organometallics*, 2001, **20**, 2425–2427.
99 A. Nagai, T. Murakami, Y. Nagata, K. Kokado and Y. Chujo, *Macromolecules*, 2009, **42**, 7217–7220.
100 M. Miyata, N. Matsumi and Y. Chujo, *Polym. Bull.*, 1999, **42**, 505–510.
101 A. Lorbach, M. Bolte, H. Li, H.-W. Lerner, M. C. Holthausen, F. Jäkle and M. Wagner, *Angew. Chem., Int.Ed.*, 2009, **48**, 4584–4588.
102 N. Matsumi, K. Naka and Y. Chujo, *J. Am. Chem. Soc.*, 1998, **120**, 10776–10777.
103 N. Matsumi, T. Umeyama and Y. Chujo, *Polym. Bull.*, 2000, **44**, 431–436.
104 A. Sundararaman, M. Victor, R. Varughese and F. Jäkle, *J. Am. Chem. Soc.*, 2005, **127**, 13748–13749.
105 F. Matsumoto, Y. Nagata and Y. Chujo, *Polym. Bull.*, 2005, **53**, 155–160.
106 A. Nagai, K. Kokado, Y. Nagata and Y. Chujo, *Macromolecules*, 2008, **41**, 8295–8298.
107 A. Nagai, J. Miyake, K. Kokado, Y. Nagata and Y. Chujo, *J. Am. Chem. Soc.*, 2008, **130**, 15276–15278.
108 V. R. Donuru, G. K. Vegesna, S. Velayudham, S. Green and H. Liu, *Chem. Mater.*, 2009, **21**, 2130–2138.
109 G. Meng, S. Velayudham, A. Smith, R. Luck and H. Liu, *Macromolecules*, 2009, **42**, 1995–2001.
110 Y. Nagata and Y. Chujo, *Macromolecules*, 2007, **40**, 6–8.
111 Y. Tokoro, A. Nagai, K. Kokado and Y. Chujo, *Macromolecules*, 2009, **42**, 2988–2993.
112 Y. Nagata and Y. Chujo, *Macromolecules*, 2008, **41**, 3488–3492.
113 H. Li and F. Jäkle, *Angew. Chem., Int. Ed.*, 2009, **48**, 2313–2316.
114 C.-H. Zhao, A. Wakamiya and S. Yamaguchi, *Macromolecules*, 2007, **40**, 3898–3900.
115 H. Li, A. Sundararaman, K. Venkatasubbaiah and F. Jäkle, *J. Am. Chem. Soc.*, 2007, **129**, 5792–5793.

